

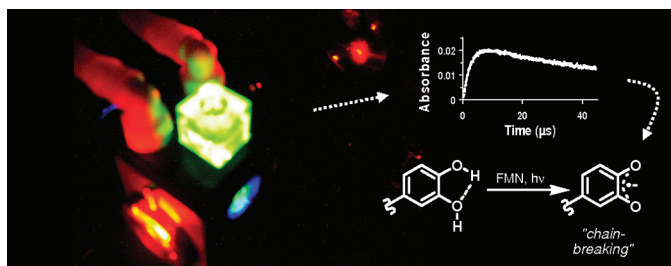
Quenching of Triplet-Excited Flavins by Flavonoids. Structural Assessment of Antioxidative Activity

Kevin Huvaere, Karsten Olsen, and Leif H. Skibsted*

Food Chemistry, Department of Food Science, Faculty of Life Sciences, University of Copenhagen, Rolighedsvej 30, DK-1958 Frederiksberg C, Denmark

ls@life.ku.dk

Received June 17, 2009



The mechanism of flavin-mediated photooxidation of flavonoids was investigated for aqueous solutions. Interaction of triplet-excited flavin mononucleotide with phenols, as determined by laser flash photolysis, occurred at nearly diffusion-controlled rates ($k \sim 1.6 \times 10^9 \text{ L mol}^{-1} \text{ s}^{-1}$ for phenol at pH 7, 293 K), but protection of the phenolic function by methylation inhibited reaction. Still, electron transfer was proposed as the dominating mechanism due to the lack of primary kinetic hydrogen/deuterium isotope effect and the low activation enthalpy ($< 20 \text{ kJ mol}^{-1}$) for photooxidation. Activation entropy worked compensating in a series of phenolic derivatives, supporting a common oxidation mechanism. An *ortho*-hydroxymethoxy pattern was equally reactive ($k \sim 2.3 \times 10^9 \text{ L mol}^{-1} \text{ s}^{-1}$ for guaiacol at pH 7) as compounds with *ortho*-dihydroxy substitution ($k \sim 2.4 \times 10^9 \text{ L mol}^{-1} \text{ s}^{-1}$ for catechol at pH 7), which are generally referred to as good antioxidants. This refutes the common belief that stabilization of incipient phenoxyl radicals through intramolecular hydrogen bonding is the driving force behind the reducing activity of catechol-like compounds. Instead, such bonding improves ionization characteristics of the substrates, hence the differences in reactivity with (photo)oxidation of isolated phenols. Despite the similar reactivity, radicals from *ortho*-dihydroxy compounds are detected in high steady-state concentrations by electron paramagnetic resonance (EPR) spectroscopy, while those resulting from oxidation of *ortho*-hydroxymethoxy (or isolated phenolic) patterns were too reactive to be observed. The ability to deprotonate and form the corresponding radical anions at neutral pH was proposed as the decisive factor for stabilization and, consequently, for antioxidative action. Thus, substituting other ionizable functions for the *ortho*- or *para*-hydroxyl in phenolic compounds resulted in stable radical anion formation, as demonstrated for *para*-hydroxybenzoic acid, in contrast to its methyl ester.

Introduction

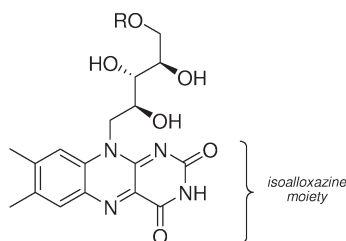
Polyphenols, as secondary metabolites, are abundant in the plant kingdom, and their structural diversity is virtually infinite. Epidemiological studies suggest that high intake of polyphenol-rich foods (fruits and vegetables) and beverages

(particularly red wine) induces beneficial health effects.^{1,2} Antioxidant activity of polyphenols has been attributed to a pivotal role herein, particularly since various pathologies have been associated with metabolic disorders that provoke excessive formation of oxidizing species (oxidative stress).

*To whom correspondence should be addressed. E-mail: ls@life.ku.dk. Phone: + 45 35 33 32 21. Fax: + 45 35 33 33 44.

(1) Scalbert, A.; Manach, C.; Morand, C.; Rémésy, C.; Jiménez, L. *Crit. Rev. Food Sci. Nutr.* **2005**, *45*, 287–306.
(2) Renaud, S.; de Lorgeril, M. *Lancet* **1992**, *339*, 1523–1526.

CHART 1. Structures of Riboflavin and Its Congeners, Flavin Mononucleotide and Flavin Adenine Dinucleotide



Riboflavin: R=H
Flavin mononucleotide: R=P(O)(OH)O Na⁺
Flavin adenine dinucleotide: R=P(O)(OH)O-P(O)(OH)O-adenosyl

On the other hand, prevalence of polyphenols protects the food matrix itself against oxidative instability, thus reducing intake of toxic oxidation products (such as peroxides) and provoking an indirect health benefit.³ Putative molecular culprits in the mentioned oxidation reactions are, among others, superoxide ($O_2^{\bullet-}$), as precursor for the reactive hydroperoxyl radical (HOO^{\bullet}), hydroxyl radicals (HO^{\bullet}) produced by Fenton chemistry, and lipid-derived peroxy radicals (ROO^{\bullet}). Radical attack accounts for breakdown of biomolecules, but also singlet oxygen (1O_2), a nonradical reactive oxygen species, induces harmful peroxide ($ROOH$) formation.^{4–6} Singlet oxygen is generated from various sources, of which photosensitization (so-called type II photooxidation) has been extensively studied. Suitable sensitizers, such as riboflavin (vitamin B₂), flavin mononucleotide (FMN), and flavin adenine dinucleotide (FAD) (Chart 1), are endogenous, as they prevail in the cellular respiration cycle and act as important cofactors or are present as essential nutrients (as in dairy products). Their photoreactivity is due to the isoalloxazine moiety, which accounts for absorption maxima around 375 and 445 nm.⁷ Exposure to UV-A (from ~320 to ~400 nm) or to blue light yields a singlet-excited state, which undergoes efficient intersystem crossing to triplet-excited flavin. Besides transferring energy to molecular oxygen to produce 1O_2 , the triplet state acts as a powerful oxidant ($E \sim 1.7$ V) capable of oxidizing various organic compounds (type I photooxidation).⁸ Cellular structures have been found to be sensitive to light exposure, and reaction products of flavin-mediated photo-reactions of tyrosine and tryptophan residues were found to be lethal to human and mammalian cells.^{9,10} Moreover, promutagenic DNA lesions were detected in the genomic sequence after exposing flavin-enriched mammalian cells to

light,^{11–13} but damage could be inhibited by vitamin C.¹⁴ Likewise, antioxidative properties of vitamin E and related model compounds (Trolox) were reported to deactivate pivotal triplet-excited flavins.^{15–17} Still, physiological concentrations of vitamins C and E are limited, but the intake of supplementary antioxidants such as flavonoids (an important subclass of the polyphenol series) through particular diets possibly assists in inhibiting biological damage caused by photogenerated oxidizing species.^{18–21} A similar mechanism was accordingly suggested for protection of light-exposed foods and beverages.^{22,23}

Since reactive triplet-excited flavin was considered to be a pivotal intermediate in both type I and type II photooxidation reactions, the possibility of its quenching by flavonoids was investigated. Insight in the quenching mechanism was the aim, and therefore, a systematic set of relevant flavonoids was subjected to a series of kinetic experiments involving laser flash photolysis. To determine whether hydrogen abstraction or electron transfer accounted for quenching, the occurrence of a kinetic isotope effect was investigated and activation parameters were calculated. Radical intermediates were identified by electron paramagnetic resonance (EPR) spectroscopy, but only after generation of detectable steady-state concentrations. Eventually, results were combined to propose a molecular explanation that contributes to the general understanding of antioxidative activity and particularly to the protection against light-induced damage.

Results

Kinetic Analyses of Flavonoid Photooxidation. Reactivity of flavonoids toward short-lived triplet-excited flavin molecules was investigated in a set of kinetic analyses based on laser flash photolysis coupled to transient absorption spectroscopy. Flavin mononucleotide was preferred as light-absorbing species, as the phosphate moiety increased solubility without compromising photochemical properties. However, due to poor solubility of various substrates, buffer solutions were mixed with acetonitrile. The significant absorption of flavon-3-ol compounds (for structures, see Chart 2) in the near-UV-A region led to the choice of a 440 nm laser pulse as excitation source. Subsequent transient absorption spectroscopy produced time-resolved spectra in which the band around 720 nm was exclusively attributed to triplet-excited flavin mononucleotide ($^3FMN^*$) (Figure 1). Its lifetime, monitored at the respective wavelength, followed an exponential decay and was significantly reduced in the presence of the selected substrates (Figure 2). The observed pseudo-first-order rate

(3) Aruoma, O. I. *Food Chem. Toxicol.* **1994**, *32*, 671–683.
 (4) Davies, M. J. *Biochem. Biophys. Res. Commun.* **2003**, *305*, 761–770.
 (5) Wright, A.; Hawkins, C. L.; Davies, M. J. *Free Radical Biol. Med.* **2003**, *34*, 637–647.
 (6) Girotti, A. W. *J. Lipid Res.* **1998**, *39*, 1529–1542.
 (7) Grodowski, M. S.; Veyret, B.; Weiss, K. *Photochem. Photobiol.* **1977**, *26*, 341–352.
 (8) Sun, M.; Moore, T. A.; Song, P.-S. *J. Am. Chem. Soc.* **1972**, *94*, 1730–1740.
 (9) Nixon, B. T.; Wang, R. J. *Photochem. Photobiol.* **1977**, *26*, 589–593.
 (10) Stoien, J. D.; Wang, R. J. *Proc. Natl. Acad. Sci. U.S.A.* **1974**, *71*, 3961–3965.
 (11) Besaratinia, A.; Kim, S.-I.; Bates, S. E.; Pfeifer, G. P. *Proc. Natl. Acad. Sci. U.S.A.* **2007**, *104*, 5953–5958.
 (12) Drobetsky, E. A.; Turcotte, J.; Châteauneuf, A. *Proc. Natl. Acad. Sci. U.S.A.* **1995**, *92*, 2350–2354.
 (13) Hiraku, Y.; Ito, K.; Hirakawa, K.; Kawanishi, S. *Photochem. Photobiol.* **2007**, *83*, 205–212.

(14) Pflaum, M.; Kielbassa, C.; Garmyn, M.; Epe, B. *Mutat. Res.* **1998**, *408*, 137–146.
 (15) McVean, M.; Liebler, D. C. *Mol. Carcinog.* **1999**, *24*, 169–176.
 (16) Cardoso, D. R.; Olsen, K.; Skibsted, L. H. *J. Agric. Food Chem.* **2007**, *55*, 6285–6291.
 (17) Gutiérrez, I.; Criado, S.; Bertolotti, S.; García, N. A. *J. Photochem. Photobiol. B* **2001**, *62*, 133–139.
 (18) Kullavanijaya, P.; Lim, H. W. *J. Am. Acad. Dermatol.* **2005**, *52*, 937–958.
 (19) Sies, H.; Stahl, W. *Annu. Rev. Nutr.* **2004**, *24*, 173–200.
 (20) Swindells, K.; Rhodes, L. E. *Photodermatol. Photoimmunol. Photomed.* **2004**, *20*, 297–304.
 (21) F'guyer, S.; Afaq, F.; Mukhtar, H. *Photodermatol. Photoimmunol. Photomed.* **2003**, *19*, 56–72.
 (22) Becker, E. M.; Cardoso, D. R.; Skibsted, L. H. *Eur. Food Res. Technol.* **2005**, *221*, 382–386.
 (23) Cardoso, D. R.; Olsen, K.; Møller, J. K. S.; Skibsted, L. H. *J. Agric. Food. Chem.* **2006**, *54*, 5630–5636.

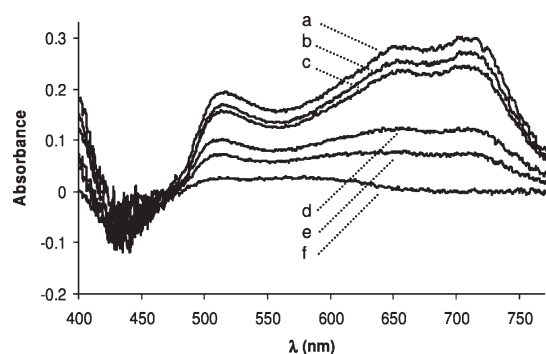


FIGURE 1. Transient absorption spectra of triplet-excited flavin recorded 0.1 μs (a), 0.5 μs (b), 1 μs (c), 5 μs (d), 10 μs (e), and 100 μs (f) after the excitation pulse.

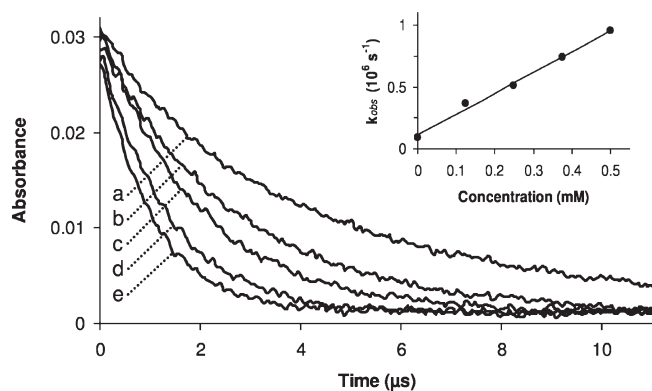


FIGURE 2. Transient absorption traces of triplet-excited flavin mononucleotide ($^3\text{FMN}^*$), observed at 720 nm, in the presence of varying concentrations of catechin, (a) 0 μM , (b) 125 μM , (c) 250 μM , (d) 375 μM , (e) 500 μM , at pH 7.0. Inset: Linear plot of the observed pseudo-first-order rate constants for the decay of $^3\text{FMN}^*$ as a function of the concentration of catechin. The nonzero intercept corresponds to the triplet lifetime in the absence of quenchers.

constants for quenching (k_{obs}) increased proportional to the polyphenol concentration, thus corresponding second-order rate constants were obtained from the slope of the resulting plot (Figure 2, inset). Except for flavanone, reaction rates were high (corresponding to rate constants $\sim 10^9 \text{ L mol}^{-1} \text{ s}^{-1}$) and not strongly affected by pH change (Table 1). However, kinetic monitoring of flavon-3-ol reactions at high pH was hindered, probably as a result of autoxidation reactions. Oxidation in the presence of an *ortho*-dihydroxy or an *ortho*-hydroxymethoxy pattern was generally faster than for isolated phenols, which was confirmed by the analysis of model systems (Table 2; for structures, see Chart 3). Furthermore, the lack of phenolic function, as in chromanone and anisole, failed to provoke quenching and concurred with the findings for flavanone.

Hydrogen Abstraction versus Electron Transfer. Oxidation reactions of (poly)phenolic compounds have been previously associated with hydrogen atom abstraction from a phenolic function or with electron transfer followed by proton migration from the resulting (poly)phenol radical cation. Although the net result of both mechanisms is identical, the reaction pathways are determined by different thermodynamic and kinetic properties. One-step hydrogen atom abstraction mainly depends on the bond dissociation energy (BDE) and is hampered by hydrogen bonding. On the

TABLE 1. Second-Order Rate Constants k ($10^9 \text{ L mol}^{-1} \text{ s}^{-1}$)^a for the Interaction of Flavonoids with Triplet-Excited Flavin Mononucleotide in Aqueous Buffer Mixed with Acetonitrile

compound	pH				
	4.2	5.4	7.0	8.5	10.0
flavanone	nq ^b	/ ^c	nq	/	nq
chrysin	1.0	1.0	0.8	1.0	0.9
naringenin	1.2	1.1	1.0	1.1	1.1
apigenin	1.1	/	1.1	/	/
kaempferol	1.5	/	1.3	/	x ^d
luteolin	2.0	/	2.0	/	/
quercetin	1.9	2.0	1.9	1.2	x
rutin ^e	1.4	/	1.2	/	x
catechin ^e	1.8	1.6	1.6	1.3	1.6

^aExperimental error on reported values is $\leq 10\%$. ^bNo quenching observed. ^cNot determined. ^dData collection hampered by instability of compounds at high pH. ^e 1.0×10^9 and $1.4 \times 10^9 \text{ L mol}^{-1} \text{ s}^{-1}$ for the interaction of rutin and catechin with triplet-excited riboflavin, respectively, in a mixture of acetonitrile and pH 6.8 buffer (see ref 22).

TABLE 2. Second-Order Rate Constants k ($10^9 \text{ L mol}^{-1} \text{ s}^{-1}$)^a for the Interaction of Selected Phenol Derivatives with Triplet-Excited Flavin Mononucleotide in Aqueous Buffer Mixed with Acetonitrile (Oxidation Peak Potentials, E_p (Expressed in V vs SHE), Determined in Acetonitrile)

compound	pH					E_p
	4.2	5.4	7.0	8.5	10.0	
	phenol derivatives					
phenol ^b	1.7	1.7	1.6	1.4	1.6	1.67
anisole	/ ^c	/	nq ^d	/	/	2.01
catechol	2.8	2.3	2.4	2.1	2.0	1.23
guaiacol ^e	2.5	/	2.3	/	2.6	1.39
2',4'-DHP ^f	0.8	/	0.8	/	1.4	/
5-MR ^g	1.9	/	1.8	/	1.8	/
chromanone	nq	/	nq	/	nq	/

^aExperimental error on reported values is $\leq 10\%$. ^b $0.5 \times 10^9 \text{ L mol}^{-1} \text{ s}^{-1}$ for the interaction with triplet-excited riboflavin in methanol (see ref 24). ^cNot determined. ^dNo quenching observed. ^e $2.6 \times 10^9 \text{ L mol}^{-1} \text{ s}^{-1}$ for the interaction with triplet-excited riboflavin in a mixture of acetonitrile and pH 4.6 buffer (see ref 23). ^f2',4'-Dihydroxypropiophenone. ^g5-Methoxyresorcinol.

contrary, electron transfer, determined by the substrate's ionization potential (IP), is favored in protic solvents due to stabilization of charged intermediates. In an attempt to identify the major pathway in flavin-mediated photooxidation of phenolic compounds, the occurrence of a primary kinetic isotopic effect ($k_{\text{H}}/k_{\text{D}}$) was investigated. Photooxidation rate constants obtained for phenol and phenol- d_6 (1.5×10^9 and $1.1 \times 10^9 \text{ L mol}^{-1} \text{ s}^{-1}$, respectively) resulted in a small $k_{\text{H}}/k_{\text{D}}$ of 1.4. Hydrogen transfer is thus refuted, a result that concurs with the information extracted from activation parameters that were calculated according to the Eyring equation (eq 1). Activation enthalpy (ΔH^\ddagger) of phenol and derivatives (Table 3 and Figure 3) was relatively low and in agreement with electron transfer rather than a process of bond breaking and bond formation in the transition state. Slightly higher values were observed for catechol-like structures, most likely because oxidation involves breaking of an intramolecular hydrogen bond. Negative activation entropies (ΔS^\ddagger) accommodate major solvent rearrangements in

(24) Haggi, E.; Bertolotti, S.; Garcia, N. A. *Chemosphere* **2004**, *55*, 1501–1507.

TABLE 3. Activation Parameters Calculated for the Interaction of a Series of Phenolic Compounds with Triplet-Excited Flavin Mononucleotide in Phosphate Buffer (pH 7) Mixed with Acetonitrile (1:1, v/v)

compound	ΔH^\ddagger (kJ mol ⁻¹)	ΔS^\ddagger (J K ⁻¹ mol ⁻¹)
phenol	8.7 ± 0.5	-39 ± 2
catechol	16.1 ± 1.4	-11 ± 5
chrysin	12.3 ± 2.0	-31 ± 7
naringenin	10.5 ± 3.3	-35 ± 11
catechin	11.6 ± 3.6	-29 ± 12
quercetin	13.8 ± 3.3	-20 ± 11

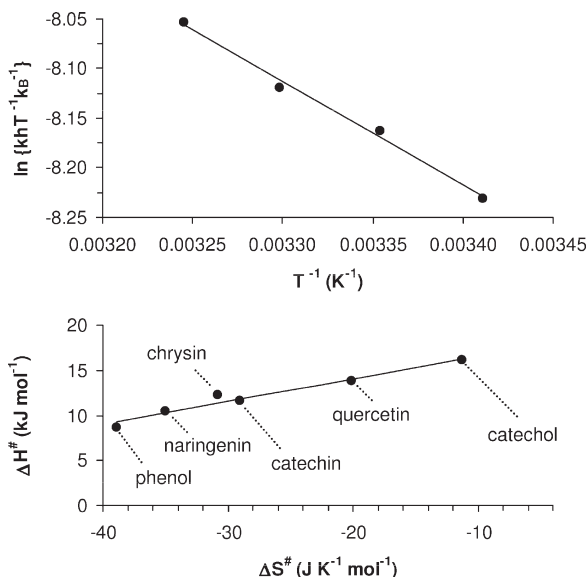


FIGURE 3. Top panel: Eyring plot for the oxidation of phenol by triplet-excited flavin mononucleotide (³FMN*) in a mixture of phosphate buffer (pH 7.0) and acetonitrile (1:1, v/v). Bottom panel: Isokinetic plot for the deactivation of ³FMN* by various phenolic compounds.

the transition state and corroborate solvent-assisted electron transfer followed by proton exchange. Entropy control was more pronounced in substrates lacking a catechol unit, resulting in a compensation effect (Figure 3). The latter supports a common oxidation mechanism for the investigated compounds.

$$\ln\left(\frac{k \times h}{T \times k_B}\right) = \frac{\Delta S^\ddagger}{R} - \frac{\Delta H^\ddagger}{RT} \quad (1)$$

Polyphenol-Derived Radicals. Electron transfer eventually produced polyphenol-derived radical intermediates, but the detection window for transient absorption spectroscopy was narrowed by the accumulated absorption of the flavin triplet state and its reduced radical, FMNH* (pK_a ~ 8.3),²⁵ in the 500–730 nm region and flavin photobleaching around 440 nm (ground state absorption) (Figure 1). Still, radical formation from flavon-3-ol derivatives such as quercetin and rutin, with maximum absorption around 485 nm, was readily observed (Figure 4). It should be noted that detection of radicals by electron paramagnetic resonance spectroscopy is more informative, but response time is generally too slow to detect short-lived intermediates. However, substitution of a

(25) Heelis, P. F.; Parsons, B. J.; Phillips, G. O.; McKellar, J. F. *Photochem. Photobiol.* **1978**, *28*, 169–173.

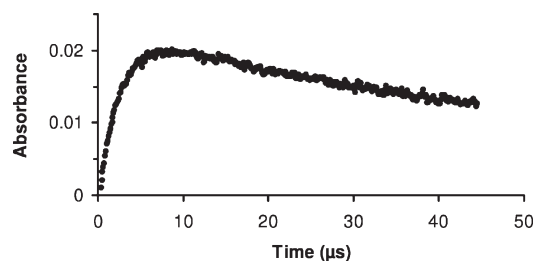


FIGURE 4. Formation and decay of the quercetin radical, measured at 485 nm, after flash photolysis of a mixture of flavin mononucleotide and quercetin in buffer (pH 4.2) mixed with acetonitrile (1:1, v/v).

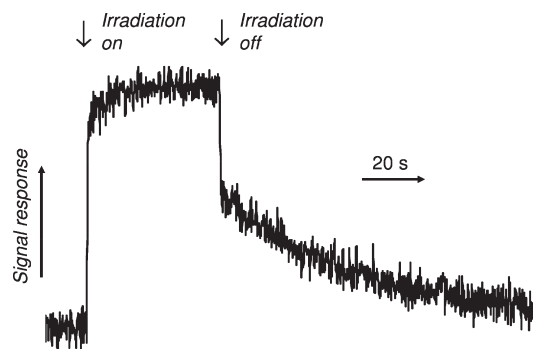


FIGURE 5. EPR trace measured in time sweep mode at static magnetic field during irradiation of a mixture of flavin mononucleotide and rutin in buffer (pH 7.0) mixed with acetonitrile (1:1, v/v).

stationary 440 nm irradiation source for the laser flash produced detectable steady-state concentrations of radicals, as shown by changes in signal intensity (at fixed magnetic field) during irradiation of rutin at pH 7 (Figure 5). Except for quercetin, which produced weak and unresolved spectra (Figure 6), intense spectra were observed for catechol-containing flavonoids (Figure 7). Corresponding coupling constants, presented in Table 4, were obtained from appropriate simulations. Assignment was based on literature data, but coupling to hydrogens on C_{5'} and C_{6'} (or C₅ and C₆ for caffeic acid) as proposed in Kuhnle's seminal work²⁶ has been questioned. According to van Acker et al., the highest spin density prevailed at C_{5'}, and consequently, C_{5'}-H was associated with the largest coupling constant.²⁷ However, the radical from a catechin derivative that has C_{6'} occupied only produced two small coupling constants (2 × 1.1 G) assigned to C_{2'}-H and C_{5'}-H.²⁸ Hence, the original identification according to Kuhnle, with C_{6'}-H accounting for major coupling, was followed.

(26) Kuhnle, J. A.; Windle, J. J.; Waiss, A. C. *J. Chem. Soc. B* **1969**, 613–616.

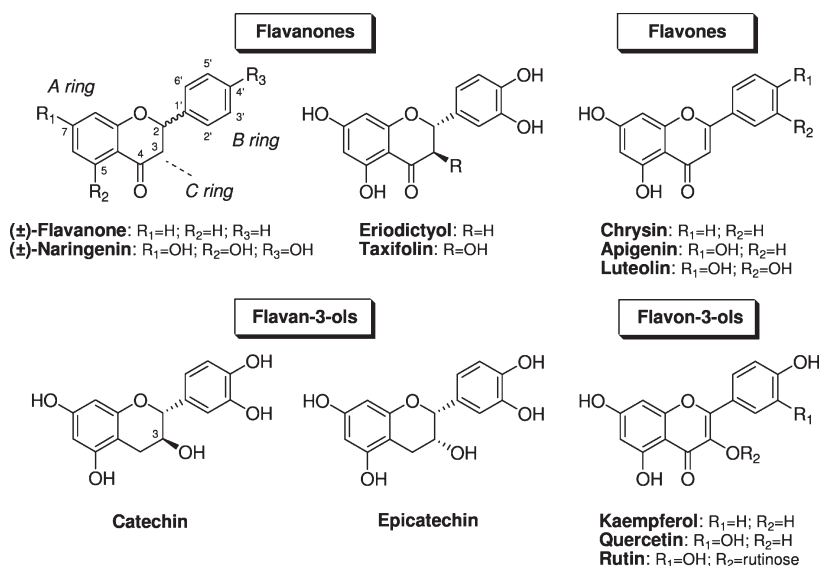
(27) van Acker, S. A. B. E.; de Groot, M. J.; van den Berg, D.-J.; Tromp, M. N. J. L.; Donné-Op den Kelder, G.; van der Vijgh, W. J. F.; Bast, A. *Chem. Res. Toxicol.* **1996**, *9*, 1305–1312.

(28) Fukuhara, K.; Miyata, N.; Ikota, N.; Fukuzumi, S.; Nakanishi, I.; Shimada, T.; Ohkubo, K.; Miyazaki, K.; Hakamata, W.; Urano, S.; Ozawa, T.; Okuda, H. *Chem. Res. Toxicol.* **2003**, *16*, 81–86.

(29) Tomkiewicz, M.; Goren, A.; Cocivera, M. *J. Am. Chem. Soc.* **1971**, *93*, 7102–7103.

(30) Adams, M.; Blois, M. S.; Sands, R. H. *J. Chem. Phys.* **1958**, *28*, 774–776.

CHART 2. Structures of Flavonoids Investigated in This Study



Contrary to quercetin, its C_3 -glycoside rutin generated intense signals which included coupling to the three remaining B-ring hydrogens. Although invisible in this spectrum, spin density was delocalized along the C_2 – C_3 unsaturation, as demonstrated by the C_3 –H coupling in the luteolin-derived radical. On the other hand, flavanones and flavan-3-ols showed an extra coupling to C_2 –H on the C-ring, the magnitude of which was strongly variable. The trans-disposition of C_3 –OH (in reference to C_2 –aryl) in catechin and taxifolin resulted in a relatively small coupling compared to epicatechin (*cis*-OH). The dihedral angle θ , determined between the C_2 –H bond and the radical p_z -orbital (which is perpendicular to the plane of the B-ring), is directly related

to the magnitude of the respective coupling constant via the McConnell equation ($a_H \sim \cos^2 \theta$).³⁹ The smaller θ in the eriodictyol radical, as concluded from comparing its optimized geometry with that of the taxifolin radical, corroborates the higher coupling constant (Figure 8).

For compounds that lack a catechol ring, apigenin produced detectable radicals, but no spectra were observed for naringenin and kaempferol. Still, the interpretation of the apigenin spectrum was confusing, as the spectrum was strikingly similar to that of luteolin. Furthermore, two radical species were detected for chrysin ($a_H \sim 1.8$ and 1.1 G and $a_H \sim 2.0$ and 3.3 G, respectively) which, obviously, could not be ascribed to radical formation in the B-ring, but they were also considerably different from the chrysin radical

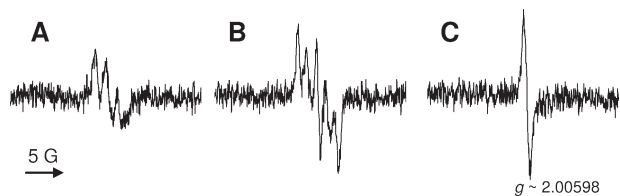


FIGURE 6. (A) EPR spectrum measured during irradiation of a mixture of flavin mononucleotide and quercetin in buffer (pH 7.0) with acetonitrile (1:1, v/v). (B,C) EPR spectra measured prior to (B) and during (C) irradiation of a mixture of flavin mononucleotide and quercetin in buffer (pH 10.0) with acetonitrile (1:1, v/v).

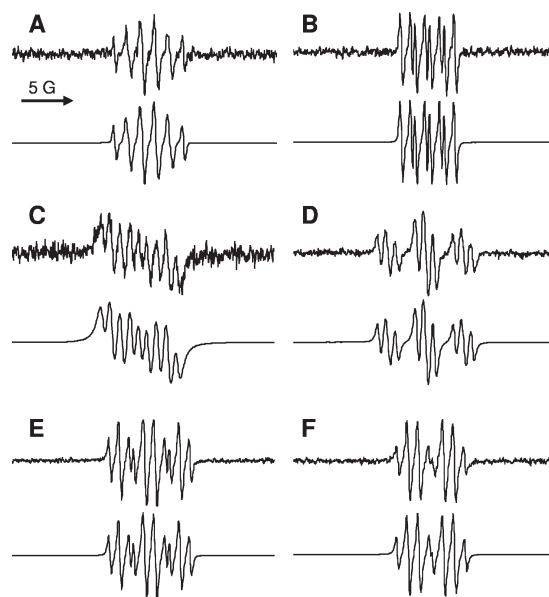


FIGURE 7. EPR spectra (top traces) and corresponding simulations (bottom traces) obtained during irradiation of polyphenols in the presence of flavin mononucleotide: (A) luteolin, (B) rutin, (C) catechin, (D) epicatechin, (E) eriodictyol, (F) taxifolin.

(31) Dixon, W. T.; Murphy, D. J. *Chem. Soc., Faraday Trans. 2* **1976**, *72*, 1221–1230.

(32) Felix, C. C.; Sealy, R. C. *J. Am. Chem. Soc.* **1982**, *104*, 1555–1560.

(33) Bors, W.; Michel, C.; Stettmaier, K.; Lu, Y.; Foo, L. Y. *Biochim. Biophys. Acta* **2003**, *1620*, 97–107.

(34) Cotelle, N.; Bernier, J.-L.; Catteau, J.-P.; Pommery, J.; Wallet, J.-C.; Gaydou, E. M. *Free Radical Biol. Med.* **1996**, *20*, 35–43.

(35) Bors, W.; Michel, C.; Stettmaier, K.; Heller, W. In *Natural Antioxidants. Chemistry, Health Effects, and Applications*; Shahidi, F., Ed.; AOCS Press: Champaign, IL, 1996; pp 346–357.

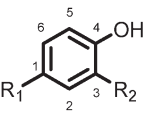
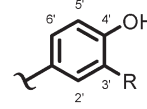
(36) Le Nest, G.; Caille, O.; Woudstra, M.; Roche, S.; Burlat, B.; Belle, V.; Guigliarelli, B.; Lexa, D. *Inorg. Chim. Acta* **2004**, *357*, 2027–2037.

(37) Bors, W.; Michel, C.; Stettmaier, K. *Arch. Biochem. Biophys.* **2000**, *374*, 347–355.

(38) Jensen, O. N.; Pedersen, J. A. *Tetrahedron* **1983**, *39*, 1609–1615.

(39) Babcock, G. T.; El-Deeb, M. K.; Sandusky, P. O.; Whittaker, M. M.; Whittaker, J. W. *J. Am. Chem. Soc.* **1992**, *114*, 3727–3734.

TABLE 4. Coupling Constants (in Gauss) and Resonance Parameters of Radicals Generated by Irradiation of Phenolic Model Compounds and Polyphenols in the Presence of Flavin Mononucleotide Compared to Reference Values

Compounds		a_H^a					g^b	SI ^c	MA ^d	Ref ^e	
		[C ₁]	[C ₂]	[C ₃]	[C ₅]	[C ₆]					
	Phenol	-	-	2.4	2.4	2.3	2.4	2.00383	0.11	0.25	tw
	Hydroquinone	-	-	2.4	2.4	2.4	2.4	2.00394	-	x	29
	Catechol	-	-	2.4	2.4	2.4	2.4	2.00469	-	x	30
		-	-	2.4	2.4	2.4	2.4	2.00455	-	x	31
		-	3.6	0.8	-	0.8	3.6	2.00393	0.30	0.25	tw
		-	3.7	0.8	-	0.8	3.7	2.0045	-	x	32
		-	3.7	0.8	-	0.8	3.7	2.00447	-	x	31
	4-HBA ^g	-	-	2.1	2.4	2.4	2.6	2.00390	-	1	tw
	3,4-DHBA ^h	-	-	1.3	-	0.8	3.2	2.00406	0.38	0.25	tw
	Caffeic acid ⁱ	0.3/2.4	-	1.3	-	1.3	2.8	2.00344	0.70	0.25	tw
	0.2/2.5	-	1.2	-	1.4	2.8	x	-	0.40	33	
		[C ₂]	[C ₃]	[C _{2'}]	[C _{3'}]	[C _{5'}]	[C _{6'}]				
	Apigenin	-	1.4	1.4	-	1.1	2.5	2.00397	-	1	tw
	Luteolin	-	1.3	1.5	-	1.1	2.6	2.00402	0.44	0.25	tw
		-	1.3	1.6	-	1.4	2.6	x	-	var	26
		-	1.0	1.8	-	3.3 ^j	1.8	x	-	1	27
		-	1.3	1.2	-	1.4	2.6	x	-	var	34
	Rutin	-	-	1.4	-	1.0	2.8	2.00388	0.11	0.25	tw
		-	-	0.9	-	2.4 ^j	0.9	x	-	1	27
		-	-	1.0	-	1.1	3.0	x	-	x	35
	Eriodictyol	2.3	-	1.0	-	0.9	3.4	2.00404	0.33	0.25	tw
		2.3	-	1.2	-	1.1	3.4	x	-	var	26
	Taxifolin	1.1	-	1.1	-	0.9	3.4	2.00396	0.20	0.25	tw
		1.2	-	1.2	-	1.1	3.4	x	-	var	26
		1.3	-	1.1	-	3.3 ^j	1.1	x	-	1	27
		0.8	-	1.2	-	3.6	2.7	2.004	-	x	36
	Catechin	1.9	-	0.8	-	1.0	3.5	2.00387	[0.33]	0.50	tw
		1.9	-	1.2	-	1.1	3.5	x	-	var	26
		1.8	-	1.1	-	2.4 ^j	1.1	x	-	1	27
		1.6	-	3.1	-	3.9	3.6	2.004	-	x	36
	2.6	-	0.8	-	0.8	2.6	x	-	0.50	37	
	1.9	-	1.1	-	1.2	3.5	2.00445	-	x	38	
Epicatechin	3.6	-	0.7	-	0.9	3.7	2.00375	[0.30]	0.50	tw	
	4.3	-	3.8	-	4.3	0.6	2.004	-	x	36	
	3.6	-	0.8	-	0.8	3.6	x	-	0.50	37	

^aCoupling with hydrogen attached to the respective carbon atom. Values from literature sources were given at 0.1 G accuracy. ^b g value ($x =$ not given). ^cSpectral intensity, as referred to the intensity of the spectrum of an aqueous 2.0 μ M TEMPO solution. Catechin and epicatechin intensities were only compared mutually due to nonlinearity between signal intensity and modulation amplitude. ^dModulation amplitude in Gauss (var. = variable, $x =$ not given). ^eReferences [in order of appearance; *tw*: this work, i.e., flavin-mediated photooxidation in a mixture of phosphate buffer (pH 7) and acetonitrile (1:1, v/v); 29: photolysis of alkaline solution; 30: quinone reduction with metallic zinc in alkaline solution; 31: cerium(IV) oxidation; 32: photolysis of aqueous solution; 33: alkaline autoxidation at pH 9.5; 26: autoxidation in DMSO/aqueous sodium hydroxide (4:1); 27: alkaline autoxidation at pH 13; 34: alkaline autoxidation by addition of NaOH; 35: enzymatic oxidation (horse radish peroxidase) at pH 8.5; 36: in situ electrolysis in aqueous Tris buffer/DMSO (1:1, v/v) in the presence of zinc acetate; 37: enzymatic oxidation (horse radish peroxidase) at pH 9.0; 38: alkaline autoxidation at pH 12.7 in aqueous DMSO]. ^fFor the sake of uniformity, numbering of carbon atoms in model systems was arbitrarily set. Numbering in polyphenols is similar as used in Chart 2. ^g4-Hydroxybenzoic acid. ^h3,4-Dihydroxybenzoic acid. ⁱCoupling constants with the olefinic protons are listed in the first column. ^jCoupling to C_{5'} according to Kuhnle²⁶ was assigned to C_{6'} (and vice versa) by van Acker et al.²⁷ (see text).

detected after oxidation by cerium(IV).⁴⁰ In the absence of phenolic functions, like in flavanone, EPR measurements remained silent and concurred with the lack of reactivity seen in the kinetic analyses.

In an attempt to obtain practicable spectra from quercetin, so-called *spin stabilization* was applied.⁴¹ Thus, incipient *ortho*-semiquinone radicals were complexated by addition of Zn²⁺, but no stabilizing effect was observed. Spectral intensity remained invariably low for quercetin, while preceding intense signals, for example, from taxifolin, practically disappeared. Alternatively, irradiations were carried out at pH 10.0, which was reported to increase radical stability.³⁸ Thus, rutin photooxidation resulted in a very

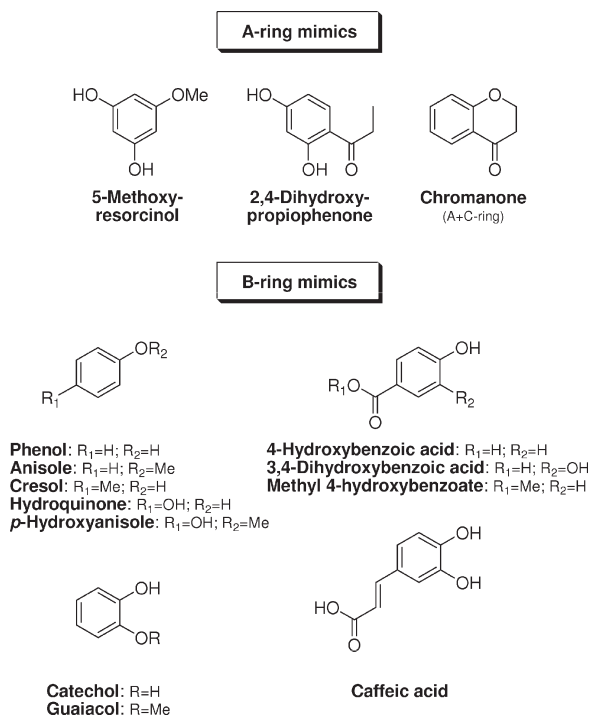
intense EPR response, although minor radical formation was already detected in the nonexposed control sample. Probably residual oxygen accounted for autoxidation, a similar problem that afflicted flash photolysis experiments. Under these conditions, radicals were also detected in unexposed quercetin solutions, but only a single line emerged during irradiation (Figure 6). From the latter experiment, it was assumed that quercetin radicals readily disappeared through interaction with ³FMN*, rather than by disproportionation.

In an attempt to characterize and confirm radical structures, relevant model compounds were investigated under identical reactions conditions (Figure 9). Phenol produced an identical spectrum as hydroquinone, but intensity of the latter was ~3 times higher. The observed coupling to four equivalent hydrogens indicated higher symmetry than the 2 × 2 coupling pattern for the regioisomer catechol. Blocking

(40) Dixon, W. T.; Moghimi, M.; Murphy, D. *J. Chem. Soc., Perkin Trans. 2* **1975**, 101–103.

(41) Stegmann, H. B.; Bergler, H. U.; Scheffler, K. *Angew. Chem., Int. Ed. Engl.* **1981**, *20*, 389–390.

CHART 3. Structures of Relevant Phenolic Models



a phenolic function, as in *p*-hydroxyanisole (methylated hydroquinone) or in guaiacol (methylated catechol), compromised radical stability, and steady-state concentrations became too low to detect. Similarly, cresol (4-methylphenol), which is an appropriate model for the B-ring in naringenin, showed only traces of radical formation during irradiation. On the other hand, a carboxyl moiety instead of a methyl group, as in 4-hydroxybenzoic acid, produced an intense EPR signal (in contrast to the methyl ester, which was EPR silent). A doubled doublet was expected when considering symmetry, but values slightly differed due to C₂–H or C₆–H interaction with the carboxylate moiety. Symmetry was lost by the extra hydroxyl in 3,4-dihydroxybenzoic acid, and three different coupling constants were observed. Basically, a similar pattern was observed for the vinylogous caffeic acid, although coupling to two conjugated methine protons introduced extra lines and raised complexity.

Spectral intensities from irradiations of 2,4-dihydroxypropiophenone or 5-methoxyresorcinol were too low to perform accurate simulations. The *meta*-substitution pattern, like in the A-ring of various flavonoids, produced highly reactive radicals that failed to build up to detectable concentrations. Chromanone, similar as flavanone, lacked reactivity due to the absence of free phenolic functions and failed to produce EPR signals.

Discussion

Pulse radiolysis, with optical spectroscopy on a sub-second time scale, has proven to be a valuable technique for obtaining mechanistic insights in behavior of radicals

(42) Bors, W.; Michel, C. *Free Radical Biol. Med.* **1999**, *27*, 1413–1426.
 (43) Bors, W.; Michel, C.; Schikora, S. *Free Radical Biol. Med.* **1995**, *19*, 45–52.
 (44) Jovanovic, S. V.; Steenken, S.; Hara, Y.; Simic, M. G. *J. Chem. Soc., Perkin Trans. 2* **1996**, 2497–2504.

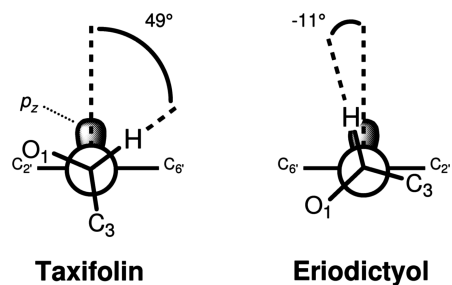


FIGURE 8. Newman projection of the C₂–C_{1'} bond in the eriodictyol radical and the taxifolin radical. The smaller dihedral angle θ between C₂–H and the p_z-orbital with unpaired spin (perpendicular to the plane of the B-ring) accounts for a higher coupling constant.

from polyphenols.^{42–46} On the other hand, characterization of incipient radicals via EPR spectroscopy provides most structural information, but the slow response of continuous-wave spectrometers is inconsistent with the fast decay of radical intermediates. Therefore, particular techniques were developed to produce steady-state concentrations of polyphenol radicals at levels detectable on EPR time scale (enzymatic oxidation, autoxidation at alkaline pH, and electrochemical oxidation),^{27,36–38} although sometimes different species than those generated by pulse radiolysis were detected.⁴⁷ The present work demonstrates that such high steady-state radical concentrations are also produced upon stationary irradiation in the presence of FMN. Moreover, since excitation of FMN by laser flash photolysis allows monitoring rise and decay of the reactive ³FMN*, reactivity of various substrates can be investigated under the same conditions. Thus, it was found that fast quenching of ³FMN* by flavonoids was slightly slower than the scavenging of hydroxyl or azidyl radicals⁴⁸ but faster than the interaction with bromide anion radicals (Br₂^{•-}) or superoxide.⁴⁵

Efficient quenching of ³FMN* ($E \sim 1.7$ V) by quercetin, a powerful antioxidant found in dietary sources such as onion and apple skin, was in agreement with its low reduction potential at physiological pH ($E_{7.4} \sim 0.3$ – 0.4 V).^{44,49} The number and favorable disposition of the hydroxyl groups, particularly the *ortho*-configuration on the B-ring, seem essential, while other structural features such as a C₂–C₃ unsaturation and, to a lesser extent, a C₄-oxo moiety also favored antioxidative activity.^{50,51} Like quercetin, the flavone luteolin complied with above-mentioned structural requirements and its low reduction potential ($E_{7.4} \sim 0.41$ V)⁴⁹ accounted for a large thermodynamic driving force. The resulting rate constants were invariably higher than the analogous apigenin ($E_{7.4} \sim 0.71$ V), which lacks the *ortho*-dihydroxy substitution in the B-ring. Rutin, a major

(45) Jovanovic, S. V.; Steenken, S.; Tosic, M.; Marjanovic, B.; Simic, M. G. *J. Am. Chem. Soc.* **1994**, *116*, 4846–4851.

(46) Jovanovic, S. V.; Hara, Y.; Steenken, S.; Simic, M. G. *J. Am. Chem. Soc.* **1995**, *117*, 9881–9888.

(47) Bors, W.; Michel, C.; Stettmaier, K. *Methods Enzymol.* **2001**, *335*, 166–180.

(48) Bors, W.; Heller, W.; Michel, C.; Saran, M. In *Free Radicals and the Liver*; Csomos, G., Feher, J., Eds.; Springer Verlag: Berlin, Germany, 1992; pp 77–95.

(49) Jørgensen, L. V.; Skibsted, L. H. *Free Radical Res.* **1998**, *28*, 335–351.

(50) Rice-Evans, C. A.; Miller, N. J.; Paganga, G. *Free Radical Biol. Med.* **1996**, *20*, 933–956.

(51) van Acker, S. A. B. E.; van den Berg, D.-J.; Tromp, M. N. J. L.; Griffioen, D. H.; van Bennekom, W. P.; van der Vijgh, W. J. F.; Bast, A. *Free Radical Biol. Med.* **1996**, *20*, 331–342.

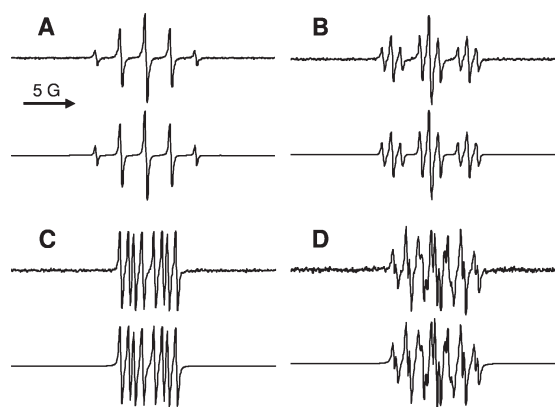
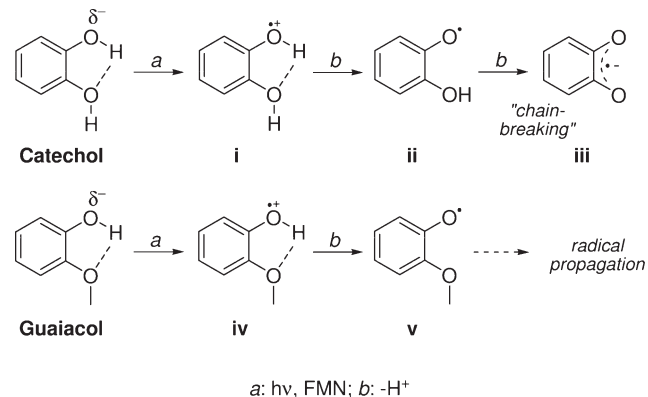


FIGURE 9. EPR spectra (top traces) and corresponding simulations (bottom traces) obtained during irradiation of phenolic model compounds in the presence of flavin mononucleotide: (A) hydroquinone, (B) catechol, (C) 3,4-dihydroxybenzoic acid, (D) caffeic acid.

quercetin glycoside (at C₃) with the same reduction potential as luteolin,⁴⁹ reacted slower, possibly due to reduced diffusion and steric effects from the bulky sugar moiety. Despite the lack of a C₂–C₃ unsaturation and C₄-oxo moiety, reactivity of catechin approached that of quercetin and luteolin. The importance of the catechol function in the quenching mechanism, as thus demonstrated, is commonly attributed to stabilization of ensuing radicals by intramolecular hydrogen bonding. However, such a stabilization pathway fails to explain the similar reactivity observed for the model compounds catechol and guaiacol, and moreover, catechol-derived radicals are readily deprotonated to the corresponding radical anion (pK_r ~ 4–5).^{45,52} Accordingly, interference of intramolecular hydrogen bonding in resulting radical intermediates is refuted, but it is more likely involved in increasing electron density on the phenolic oxygen (Scheme 1). The resulting lower ionization potential of catechol and derivatives concurs with a more efficient electron transfer toward ³FMN* (vide infra) and supports the superior reducing activity of these compounds. A comparable, albeit intermolecular, interaction (i.e., with solvent molecules) was suggested to accelerate reduction of a 2,2-diphenyl-1-picrylhydrazyl radical by phenolic compounds in alcohol compared to aprotic solvents.⁵³ The advantage of *ortho*-substitution was demonstrated after comparison with oxidation of *meta*-substituted 5-methoxyresorcinol, which occurred at rates similar to those of unsubstituted phenol. The presence of an exocyclic oxo moiety, as in 2,4-dihydroxypropiofenone, impaired oxidation, as the electron-withdrawing effect resulted in higher reduction potentials ($E_7 = 0.89$ vs 0.84 V for 5-methoxyresorcinol).^{44,46} It was therefore concluded that reactivity of the A-ring in most flavonoids was low, and interaction preferably occurred via the B-ring.^{45,54} Nevertheless, comparable rates of ³FMN* quenching were observed for chrysin (lacks B-ring hydroxyls) and apigenin, which assumed the feasibility of mixed mechanisms. Possibly, conjugation to the electron-withdrawing C₄-oxo moiety in apigenin lowered reactivity of

SCHEME 1. Hydrogen Bonding in Phenols with *ortho*-Dihydroxy or *ortho*-Hydroxymethoxy Substitution Pattern Affects Ionization Properties and Facilitates Electron Transfer toward Triplet-Excited Flavins^a



^aStabilization of phenoxyl radicals (resulting from proton loss from incipient radical cations) to corresponding radical anions is reserved to phenols with *ortho*-dihydroxy substitution.

the B-ring phenol, which, as a consequence, promoted participation of the A-ring in electron transfer. Previous observations for galangin, in which free hydroxyls on the B-ring are absent, led to the conclusion that multiple phenolic functions are involved in kinetically controlled oxidation reactions,^{44,46} followed by intramolecular hydrogen transfer to yield the thermodynamically favored radical (mostly on the B-ring). However, the mechanism remained open to question since the decay of A-ring radicals could not be correlated to B-ring radical growth.⁵⁵

Mechanistic Interpretation of Photooxidation. The nearly diffusion-controlled rate constants, in combination with the lack of kinetic isotopic effect, were strong indications of an electron transfer toward ³FMN*. As a comparison, interaction of phenol derivatives with peroxy radicals, which are weaker oxidants ($E \sim 1.0$ V⁵⁶ vs $E \sim 1.7$ V for ³FMN*), occurred by hydrogen atom abstraction ($k \sim 10^5$ – 10^6 L mol⁻¹ s⁻¹) and resulted in a $k_H/k_D \geq 4$.^{57,58} In line with the proposed electron transfer in flavin-mediated photooxidations, the rate constant for anisole was expected to be similar to that of phenol. However, O-methylation inhibited oxidation, similar to that seen for the interaction of ³FMN* with tyrosine, TyrOH ($k \sim 10^9$ L mol⁻¹ s⁻¹), and TyrOMe (no quenching).⁵⁹ The lack of labile hydrogens in the methylated substrates is obvious, but most likely inhibition followed from changes in ionization properties. The significant shift in peak potential for anisole, as indicated by cyclic voltammetry experiments in aprotic solvent (Table 2), supports this view. Most likely, incipient phenolic radical cations barely tolerate positive charge and instantly deprotonate after electron transfer, hence the absence of such

(55) Cren-Olivé, C.; Hapiot, P.; Pinson, J.; Rolando, C. *J. Am. Chem. Soc.* **2002**, *124*, 14027–14038.

(56) Buettner, G. R. *Arch. Biochem. Biophys.* **1993**, *300*, 535–543.

(57) Burton, G. W.; Doba, T.; Gabe, E.; Hughes, L.; Lee, F. L.; Prasad, L.; Ingold, K. U. *J. Am. Chem. Soc.* **1985**, *107*, 7053–7065.

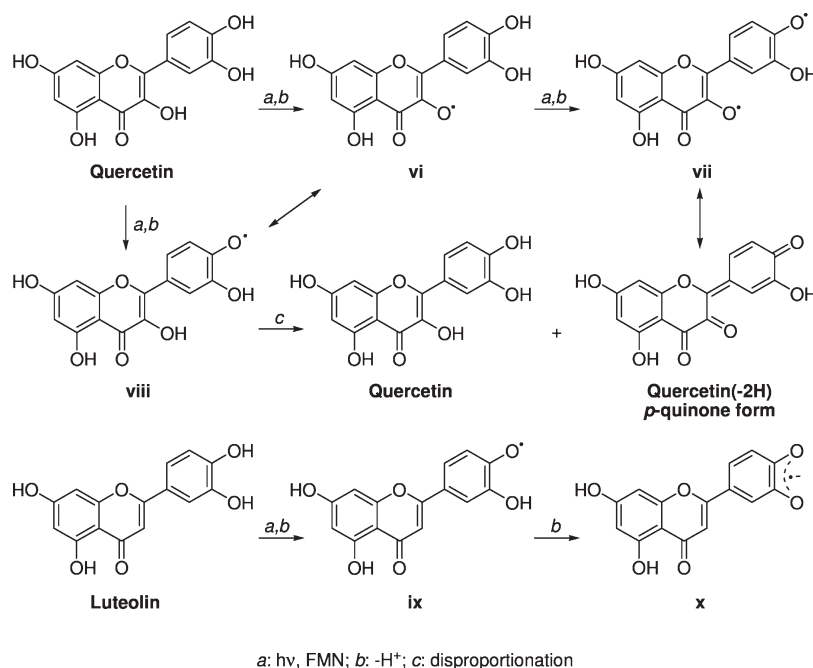
(58) Burton, G. W.; Le Page, Y.; Gabe, E. J.; Ingold, K. U. *J. Am. Chem. Soc.* **1980**, *102*, 7791–7792.

(59) Tsentelovich, Y. P.; Lopez, J. J.; Hore, P. J.; Sagdeev, R. Z. *Spectrochim. Acta A* **2002**, *58*, 2043–2050.

(52) Steenken, S.; Neta, P. *J. Phys. Chem.* **1979**, *83*, 1134–1137.

(53) Litwinienko, G.; Ingold, K. U. *J. Org. Chem.* **2003**, *68*, 3433–3438.

(54) Pannala, A. S.; Chan, T. S.; O'Brien, P. J.; Rice-Evans, C. A. *Biochem. Biophys. Res. Commun.* **2001**, *282*, 1161–1168.

SCHEME 2. Fast Disappearance of Quercetin Radicals is Ascribed to Efficient Disproportionation (minor) or Consecutive (Photo)oxidation Steps (major)^a


^aThe role of C₃-OH is pivotal because luteolin produces stable, detectable radical anions.

stabilization mechanism in anisole is suspected to inhibit (photo)oxidation.

Structural Implications for Radical Stability. Stationary irradiation at neutral pH (mixed with organic solvent) was effective in generating steady-state concentrations of polyphenolic radicals. Despite the thermodynamic control, which not necessarily yields incipient species, radical structures concurred with oxidation mechanisms suggested from kinetic data. Besides, signal intensity, as observed in EPR spectroscopy, was used for estimating radical stability since this largely determines antioxidative properties. Indeed, unstable, reactive polyphenolic radicals are difficult to detect and probably behave as chain-carrying species which propagate oxidation. On the other hand, high steady-state concentrations, as found for radicals from catechol-containing compounds, suggest excellent chain-breaking activity. Quercetin was a remarkable exception since, despite its known powerful chain-breaking properties, radicals readily disappeared from the reaction mixture. Still, quercetin analogues like luteolin (no C₃-OH) and rutin (C₃-OH protected as glycoside) furnished relatively long-lived species (for example, **x** in Scheme 2), hence disappearance of quercetin radicals was ascribed to the presence of C₃-OH. The latter probably interfered in a disproportionation step⁶⁰ or, more likely, in a consecutive electron transfer which led to formation of EPR-silent reaction products (Scheme 2). At high pH, the single line corresponds to superoxide (O₂^{•-}) formation and not to a quercetin radical as previously thought.⁶¹ A feasible mechanism for its formation involves reduction of residual oxygen by FMN^{•-} (formed by electron

transfer from quercetin to ³FMN^{*}) with regeneration of FMN. In addition, autooxidation, which is particularly effective due to the lower reduction potential of quercetin at high pH,²⁷ produces superoxide, as well.

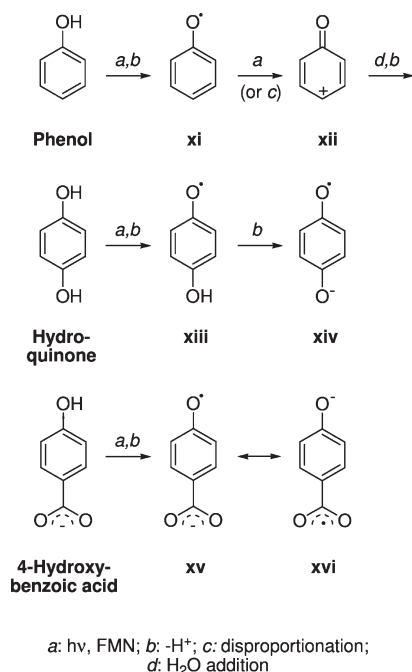
From the above-mentioned observations, the chemistry behind the favorable antioxidative properties of compounds with *ortho*- or *para*-dihydroxy substitution was assigned to fast deprotonation of incipient phenoxyl radicals to form stable radical anions at neutral or physiological pH. Model compounds like catechol and hydroquinone nicely illustrate this, particularly when compared to their mono-O-methylated derivatives (Scheme 1). Indeed, neutral phenoxyl radicals from guaiacol (**v**) or *p*-hydroxyanisole were too unstable to detect and are probably incapable of breaking the radical chain.⁶² It is worth noting that the foregoing compromises *in vivo* antioxidative activity of polyphenols, as methylation, accommodated by phase II enzymes like catechol-*O*-methyl transferase, is an important biotransformation during metabolism.⁶³ The importance of the dihydroxy pattern for stabilizing radical intermediates was seemingly contradictory to the intense signals observed during phenol irradiation. However, the resemblance to the spectrum of the *p*-benzosemiquinone radical anion (**xiv**) was striking and assumed preceding hydroquinone formation (Scheme 3), similar to that found for photolysis of phenoxide anions in alkaline solution.²⁹ The latter involved nucleophilic addition of a hydroxide anion to phenol, but such a mechanism was unlikely under the current conditions (mixed buffer at pH 7). Therefore, water addition to an intermediate phenoxonium (**xii**) was proposed, whereby the cation results from disproportionation or

(60) Dangles, O.; Fargeix, G.; Dufour, C. *J. Chem. Soc., Perkin Trans. 2* **1999**, 1387–1395.

(61) Miura, T.; Muraoka, S.; Fujimoto, Y. *Food Chem. Toxicol.* **2003**, *41*, 759–765.

(62) Lemańska, K.; van der Woude, H.; Szymusiak, H.; Boersma, M. G.; Gliszczynska-Swigło, A.; Rietjens, I. M. C. M.; Tyrakowska, B. *Free Radical Res.* **2004**, *38*, 639–647.

(63) Zhu, B. T.; Ezell, E. L.; Liehr, J. G. *J. Biol. Chem.* **1994**, *269*, 292–299.

SCHEME 3. Photooxidative Conversion of Phenol to Hydroquinone, Followed by Stable Radical Anion Formation^a


^aUnlike for hydroquinone, stable radical anion formation from 4-hydroxybenzoic acid is due to the ionized carboxylate at neutral pH.

a second photooxidation step. In this respect, the similarity between luteolin and apigenin radicals was suspected to arise from an analogous hydroxylation reaction. On the contrary, radicals from 4-hydroxybenzoic acid did not result from intermediate hydroxylation reactions (Scheme 3). The high steady-state concentrations were ascribed to formation of stable radical anions (**xv** ↔ **xvi**) instead of reactive neutral radicals (as with methyl 4-hydroxybenzoate). The conclusion that stabilization is maintained by substituting another ionizable group for one of the phenolic functions in the *ortho*- or *para*-dihydroxy pattern possibly contributes to the design of advanced antioxidants.

Conclusions

Studies on photochemical properties of flavins are numerous and cover a broad scientific area. Flavin photochemistry was previously found to be essential to blue-light-mediated signaling pathways in the plant kingdom, thus triggering electron transfer and radical cation formation in phototropins and cryptochromes. Furthermore, endogenous sensitizers in cellular matrices were activated upon exposure and resulted in cytotoxicity or damage to biomolecules. Similar processes affect food products and dietary supplements rich in vitamin B₂, leading to nutritional loss and deprived quality. The intermediate triplet-excited flavin plays a pivotal role in these phenomena due to its sensitizing properties (leading to type II photooxidation) and its high redox potential (accounting for type I oxidation). However, efficient quenching of this transient oxidant by natural antioxidants such as polyphenols allows inhibition of adverse effects associated with light exposure. Beside this, irradiation was found to be an efficient mechanistic tool for characterizing oxidized intermediates and to determine their role in the

antioxidative mechanism, particularly since control of conditions was superior to alkaline autoxidation reactions. Using this approach, it was concluded that radical anion formation from incipient neutral radicals was decisive for chain-breaking antioxidant activity. An *ortho*- or *para*-dihydroxy-substituted benzene as substructure complied and allowed formation of resonance-stabilized radical anions. Interestingly, replacing a hydroxyl by a carboxylate function maintained stabilizing activity, as concluded from the high steady-state concentration of the resulting radical anion. This provides important new insights in the chemistry behind phenolic antioxidants, but correlation with physiological benefits, such as inhibition of pathological conditions, remains difficult to predict.¹ Particularly, the limited uptake, due to fast metabolism and excretion, only results in transient polyphenol concentrations in human plasma and compromises *in vivo* activity.⁶⁴ Their role in indirect health effects, as through preserving sensitive foods from forming toxic oxidation products, is less controversial and supports a functional role for polyphenols in future food systems.

Experimental Section

Substrates (polyphenols and model compounds) of high purity (>98%) were used as such. Acetonitrile was of spectro-photometric grade, while deuterium oxide was 99.96% pure. Aqueous solutions were prepared using a Milli-Q purification device (Millipore, Bedford, MA) ($R = 18 \text{ M}\Omega \cdot \text{cm}$). Buffers at 0.10 M were freshly prepared from analytical grade chemicals, that is, acetic acid and sodium acetate (pH 4.2), citric acid and sodium citrate (pH 5.6), potassium dihydrogenphosphate and sodium hydroxide (pH 7.0), boric acid and sodium hydroxide (pH 8.5), and sodium bicarbonate and sodium hydroxide (pH 10.0).

Laser Flash Photolysis Spectroscopy. A dye laser (Spectron Laser Systems, Rugby, U.K.) containing a coumarin 440 (Exciton, Dayton, OH) solution in methanol was pumped by the third harmonic (355 nm) of a pulsed Q-switch Nd:YAG laser. The resulting 440 nm laser flash (~2.6 mJ per pulse) was guided into the cell cavity, which housed a quartz cuvette containing a nitrogen-purged solution of flavin mononucleotide (125 μM) and selected compounds (concentrations varying from 125 μM up to 5 mM) in a buffer–acetonitrile mixture (1:1, v/v). Specific reaction conditions were applied for the experiments involving kinetic isotope effects as buffer molecules were omitted from the reaction mixture, while deuterium oxide was substituted for water as solvent for photooxidations of deuterated compounds.

The analytical light beam, generated by a pulsed xenon lamp (Applied Photophysics, Leatherhead, U.K.), was sent through an optical filter (cutoff wavelength = ca. 610 nm) before reaching the sample. The analyzing light beam then passed a monochromator, and transient absorption at 720 nm was eventually measured by a R928 photomultiplier tube (Hamamatsu Photonics, Hamamatsu City, Japan). Formation and decay traces of radicals, derived from quercetin and rutin, were monitored at 485 nm (after installation of filters with appropriate cutoff wavelength). Pseudo-first-order rate constants were determined (at 293 K in a mixture of buffer pH 7.0 and acetonitrile (1:1, v/v)) for varying concentrations of polyphenols and model compounds and subsequently transferred into second-order rate constants. Temperature dependence (for calculation of activation parameters) was investigated between 293 and 313 K. Absorption spectra of excited flavin transients in

(64) Lotito, S. B.; Frei, B. *Free Radical Biol. Med.* **2006**, *41*, 1727–1746.

the wavelength region of 400–760 nm were analyzed by an optical multichannel analyzer (OMA II, EG&G, Princeton Instruments, Princeton, NJ).

Electron Paramagnetic Resonance Spectroscopy. Solutions were prepared by dissolving phenolic compounds (10 mM) and flavin mononucleotide (250 μ M) in a 1:1 mixture (v/v) of acetonitrile and aqueous buffer at pH 7.0 or at pH 10.0. Extensive degassing by purging with nitrogen was carried out before transferring the reaction mixture into a flat quartz cell. Irradiation was carried out inside the EPR resonator cavity using a focused light beam (wavelength = 440 nm, power = \sim 2 mW) generated by a Photonics Polychrome II unit (TILL Photonics, Gräfelfing, Germany).

An ECS 106 spectrometer (Bruker, Karlsruhe, Germany) was used for EPR spectroscopy. The following settings were applied: center field = 3475 G (gauss); sweep width = 40 G; microwave power = 10 mW; modulation frequency = 100 kHz; modulation amplitude was optimized according to the intensity of the signal and ranged from 0.25 to 1.0 G; conversion time = 20.48 ms; time constant = 10.24 ms; sweep time = 21 s. Spectra of radicals were the result of a four-scan accumulation. Subsequent simulation of EPR spectra, in order to determine hyperfine coupling constants, was performed by the PEST WinSIM program.⁶⁵ Radical intensities were compared to the intensity of a 2 μ M 2,2,6,6-tetramethylpiperidine 1-oxyl (TEMPO) radical solution after double integration of the respective signals (only intensities recorded at similar modulation amplitudes were compared). Rise and decay of the rutinyl radical was measured at static field (3476 G) with modulation amplitude of 1.0 G and sweep time of 168 s.

Cyclic Voltammetry. Cyclic voltammetry experiments were carried out on a BAS CV-50W voltammetric analyzer

(Bioanalytical Systems (BAS), West Lafayette, IN) using a glassy carbon electrode (BAS MF-2012) as working electrode and a platinum wire as auxiliary electrode (BAS MW-1032). Substrates (2 mM) were dissolved in a solution of 0.10 M Bu₄NBF₄ in acetonitrile, which was purified over aluminum oxide prior to use. Potentials were referenced to a nonaqueous pseudoreference electrode (BAS MF-2026), which was checked daily against the standard potential of the ferrocene/ferrocenium couple, Fc/Fc⁺. Potentials, measured at a fixed sweep rate of 100 mV s⁻¹, are reported against the standard hydrogen electrode (SHE) by using $E^\circ = +650$ mV vs SHE for the Fc/Fc⁺ couple in acetonitrile.⁶⁶ The working electrode was polished and rinsed before each measurement, while solutions were thoroughly purged with nitrogen prior to analysis.

Quantum Chemical Calculations. Geometries of radicals, resulting from hydrogen abstraction at C_{4'}-OH, were optimized for minimal energy with the semiempirical AM1 method in the MOPAC interface in the ChemOffice package (Cambridgesoft, Cambridge, MA). Thus, estimates of torsion angles between C₂-H and the p_z-orbital, perpendicular to the B-ring of the respective flavonoid radical, were made.

Acknowledgment. Financial support by Arla Foods, the Danish Dairy Research Foundation, and the Directorate for Food, Fisheries, and Agricultural Business was gratefully accepted.

Supporting Information Available: Atom coordinates and geometries of taxifolin and eriodictyol radicals. This material is available free of charge via the Internet at <http://pubs.acs.org>.

(65) Duling, D. R. *J. Magn. Reson., Ser. B* **1994**, *104*, 105–110.

(66) Daasbjerg, K.; Pedersen, S. U.; Lund, H. *General Aspects of the Chemistry of Radicals*; John Wiley & Sons: New York, 1999; pp 385–427.